Available online at www.sciencedirect.com
ScienceDirect
Journal of Power Sources 172 (2007) 422–427
JOURNAL OF POWER SOURCES
www.elsevier.com/locate/jpowsour

Short communication

WO_3 pillar-type and helical-type thin film structures to be used in microbatteries

R. Figueroa [a,*], Tersio G.S. Cruz [b], A. Gorenstein [a]

[a] *Applied Physics Department, Physics Institute, UNICAMP, CP 6165 CEP 13083-970 Campinas, SP, Brazil*
[b] *Telecommunication Technological Division, CESET/UNICAMP, CEP 13484-370 Limeira, SP, Brazil*

Received 5 May 2007; received in revised form 17 May 2007; accepted 18 May 2007
Available online 26 May 2007

Abstract

In the present study WO_3 thin films were deposited by sputtering onto ITO glass, W/ITO and Si substrates by using the glancing angle deposition (GLAD) technique, with the objective of applying these materials in electrochemical intercalation devices. The thin films microstructure and electrochemical behavior were determined through scanning electron microscopy (SEM) and cycling at constant current with potential limitation. By mainly adjusting the substrate holder speed rotation, pillar-type and helical-type structures were obtained under high and low speed rotation levels, respectively. The electrochemical results showed that the best charge capacity performance was obtained for the WO_3/W/ITO films with pillar-type structures, which are more porous.

Keywords: Tungsten oxide; Reactive sputtering; Thin films; Microbatteries

1. Introduction

There is an increased interest in new research towards the improvement on the performance of intercalated devices, such as lithium ion microbatteries [1–9]. The principle in such devices is based on the utilization of thin films as electrodes which allow for the reverse intercalation of lithium ions in their structure. Recently, in addition to the search for new materials, new thin film structures and surfaces are being explored in order to discover new properties [10–14], several with positive impact on technological applications. With this objective, our interest was to study the influence of such structures on the performance of WO_3 thin films that may be used as the cathode in microbatteries. The WO_3 material is known for its electrochemical properties of intercalation [9,15–17].

In order to obtain the required microstructures the glancing angle deposition (GLAD) technique was utilized. The technique performs oblique angle deposition (Fig. 1) while the substrate may be kept rotating at a definite speed [14,18–20]. This technique allows for the production of either pillar-type or helical-type nanometric structures. The growth of such microstructures is strongly influenced by the atomic shadowing and greatly enhanced by the limited atomic diffusion conditions [12,14,18,21–25]. One of the characteristics of the GLAD deposition technique is the production of highly porous thin film structures which offer a larger effective area for ion intercalation.

The GLAD configuration has been reported using electron beam [26] and thermal evaporation [13,18,22,25,27,28] deposition techniques. However, very few studies report deposition using the sputtering technique [20,22,27]. The reason may be related to problems deriving from the dispersion of the atoms occurring under sputtering.

In the present work a structural and morphological study was conducted in WO_3 thin films deposited via sputtering using the GLAD configuration. A simple model describes the process through which the structures are formed and a study of the electrochemical behavior of the samples through their charge capacity examination is presented.

2. Experimental

2.1. Method for cathode production

The WO_3 thin films were prepared by reactive rf magnetron sputtering system using a BAE 250 equipment. During

* Corresponding author. Tel.: +55 19 35215450; fax: +55 19 35215376.
E-mail address: rcadillo@ifi.unicamp.br (R. Figueroa).

0378-7753/$ – see front matter © 2007 Elsevier B.V. All rights reserved.
doi:10.1016/j.jpowsour.2007.05.080

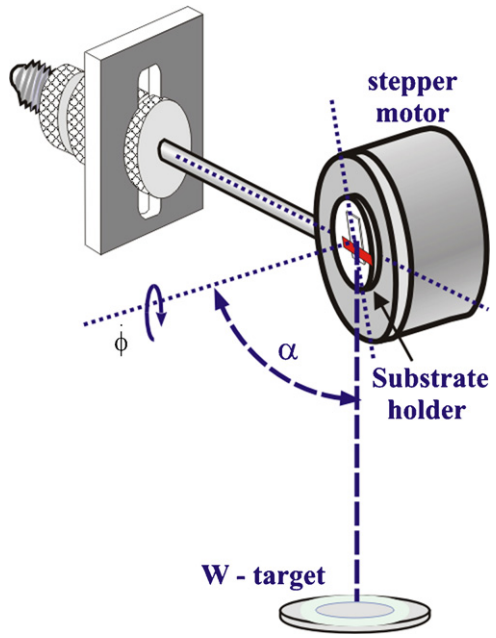

Fig. 1. Basic experimental set up for the GLAD configuration technique. A stepper motor controls rotation of the substrate holder. The stepper motor is mounted on a mechanical support so that the flux arrives at an angle α on the substrate.

deposition a W target of 2-in. diameter immersed in an Ar/O_2 reactive atmosphere was used. Si and ITO/glass substrates were, respectively utilized for SEM and electrochemical characterizations. The distance between the center of the target and the center of the substrate holder was 12 cm. The sputtering chamber was evacuated to below 3×10^{-6} mbar. Other deposition parameters are presented in Table 1. These parameters are the same as the ones utilized in the referred work [15], thus guaranteeing the amorphous characteristic and the stoichiometry of the W/O = 1/3 materials.

In order to determine thickness of the films and provide electrical contacts for electrochemical measurements, a thin, vacuum-friendly, polymeric adhesive tape was used to shield part of the substrate surface during deposition. Thickness was measured using an Alpha-Step 200 profilometer.

The experimental set up utilized for the GLAD configuration is shown in Fig. 1, where the substrate holder is manually adjusted at an inclination angle α defined by the perpendicular to the surface of the substrate holder and the vertical axis passing through the centers of both the target and the substrate holder. In spite of the occurrence of a certain degree of flux dispersion in depositions produced by sputtering, the angle of the incident flux upon the substrate was considered to be the geometric angle α, as shown in Fig. 1. The rotation of the substrate holder was controlled by a stepper motor of 1.8° resolution, positioned inside the vacuum chamber. The rotation angle ϕ revolved around the axis perpendicular to the substrate.

Table 1
Sputtering conditions for the preparation of WO_3 thin film

Deposited material	WO_3	W
Deposition angle	80°	0°
Power (Watt)	150	200
Deposition rate (τ, nm min^{-1})	20.0 ± 2.0	22.0 ± 3.0
Bias voltage (V_{DC})	-383.0 ± 5.0	-401.0 ± 5.0
Pressure (mbar)	4.5×10^{-3} ($Ar + O_2$)	4.5×10^{-3} (Ar)
Flux (sccm)	Ar: 23.3; O_2: 6.0	Ar: 35.7

Prior to the deposition of the microstructures by the GLAD technique a film was deposited onto Si and ITO/glass substrates, at an inclination angle $\alpha = 80°$, while maintaining the substrate stationary. The film micrograph produced under these conditions, shown in Fig. 2, displays columns at an inclination angle $\beta = 35.0 \pm 1.6°$, smaller than the one expected from the Tait or cosine relations [13,18,24], possibly due to the flux dispersion typically occurring in sputtering deposition.

From these preliminary results a model was built to determine the shape of the columns, by exploring the competition between the rotation speed $\dot{\phi}$ and the deposition rate τ. By supposing growth to occur solely on the superior top of the column one can determine the radius R of the helical column by using a geometric approach that defines the helical differential "dl" components, $(R\mathrm{d}\phi)$ and $(\tau \mathrm{d}t)$, Fig. 3:

$$\tan\beta = \frac{(2\pi\dot{\phi})R}{\tau} \quad (1)$$

where $\dot{\phi}$ and τ are given in rpm and nm min^{-1}, respectively. With this model it is possible to estimate the helical growth from the projections $(R\cos(2\pi\dot{\phi}t),\ \ R\sin(2\pi\dot{\phi}t), \tau t)$, where t is the duration (in min) of the film growth process. By assuming $\beta = 35°$ (experimental angle value for deposition without rotation), Fig. 2, $\tau = 20$ nm/min (Table 1) and $\dot{\phi} = 0.042$ rpm, Eq. (1) gives $R = 53$ nm, which would be the radial projection of a helical structure (Fig. 4). This helix makes a complete turn at a column height of 500 nm. For $\dot{\phi} = 36.0$ rpm (much bigger than its value in the previous configuration) the results show a degeneration of the helical-type structures into the pillar-type structures (Table 2). The build up of the pillar-type structure is caused by the tilted orientation of the flux of particles hitting the substrate which process around the axis perpendicular to the substrate at a high precession speed determined by the azimuth angle ϕ (Fig. 3.) In other words, at high speeds the flux hits the substrate uniformly for all azimuth angles ϕ in such a way that the columns are unable to grow preferentially in a particular direction.

In addition to the samples above described, other samples were prepared with ITO/glass and Si substrates in which a tungsten buffer layer (50 nm thickness and angle $\alpha = 0°$) was deposited between the substrate and the WO_3 film, Table 1, in order to improve the adherence of the WO_3 film to the substrate [29,30]. The WO_3 film deposited on top of the tungsten buffer had a pillar-type structure, characteristic of the deposition conditions displayed in Tables 1 and 2.

2.2. Morphological and microstructural characterization

In order to study the WO_3 film growth process, the morphology and the microstructure of all deposited films were examined

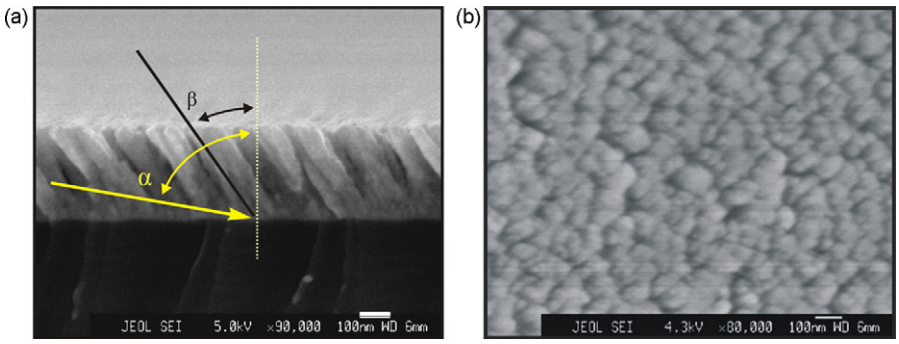

Fig. 2. (a) Deposition at an extreme oblique angle ($\alpha = 80°$), without rotation of the substrate. The angle of inclination of the columns is $\beta = 35.0 \pm 1.6°$. (b) film morphology under the conditions stated in (a).

by the scanning electron microscopy technique using a SEM-FEG 6330G apparatus. The acceleration voltage used for the samples under study was ~5 kV. The microstructure images obtained from the WO_3/Si samples cleaved with a diamond tip in liquid nitrogen. The topographic images were taken from WO_3/ITO samples.

2.3. Electrochemistry

In order to measure the charge capacity of the samples, the chronopotentiometry technique, with potential limitation, was used. The equipment utilized in the measurements was a multipotentiostate VPM (biologic). The films were prepared to have a 5 mm × 5 mm immersion area. The electrolyte used in the preparation was 1 M $LiClO_4$/PC. For both the counter-electrode and the reference electrode two metallic lithium foils were used. The experiment was performed between the potential limits 4.0–2.0 V versus Li + /Li, under a density current of 5 $\mu A\,cm^{-2}$. All the measurements were performed while keeping the electrochemical cells within a Ar-filled dry box (3.0 mbar pressure). All films were evaluated in about 50 cycles of lithium intercalation/deintercalation.

3. Results

3.1. Helical-type structures

Under the conditions in which the incident angle is kept at $\alpha = 80°$ and the rotation speed at $\dot{\phi} = 0.042$ rpm (rotation speed considered low when compared to the deposition rate) helical microstructures are formed (Fig. 5(a and b)), where the columns grow oriented in a direction close to the direction of the incidence of the adatoms, winding about the axis perpendicular to the substrate with precession speed determine by angle ϕ—a speed which is directly dependent on the rotation of the substrate holder, Fig. 3.

It is observed that the helical radius increases at each turn. However, the radius of the helical column in the first turn (47.5 nm) is close to the predicted value in Table 2. This is clearly depicted in the amplified image of Fig. 5a. The radius increment is believed to be related to the low speed rotation of the substrate and to the isolated nature of the helical columns (which display, on the top of their columns, a pattern showing two nanosurfaces, one tilted and the other parallel to the surface, Fig. 5b). These inclinations on the top of the columns allow for the radial growth of the helical structures.

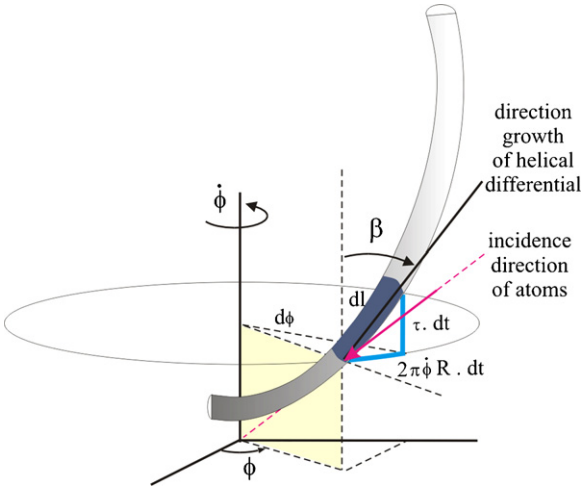

Fig. 3. Helical column formation with column radius R; deposition rate τ, and substrate rotation speed $\dot{\phi}$.

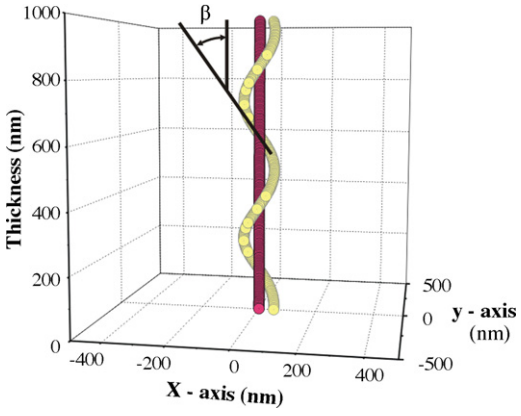

Fig. 4. Model for the pillar-type and helical-type columns, expected to be formed with the sputtering deposition technique, for the inclination angle $\beta = 35°$, without rotation of substrate, and deposition angle at $\alpha = 80°$.

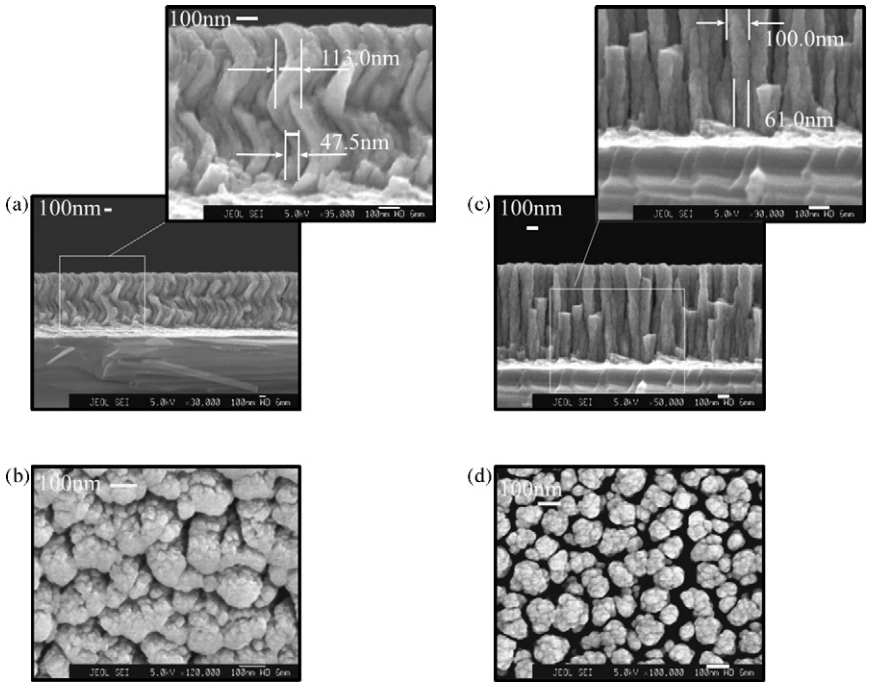

Fig. 5. WO_3/Si thin film micrographics SEM-FEG, in the 100 nm scale, for $\alpha = 80°$ e rotation speed $\dot{\phi} = 0.042$ rpm (helical): (a) transversal section of film (×30,000), with greater magnification (×95,000) for the left part of the analyzed region, (b) morphology of film (×120,000); and $\dot{\phi} = 36$ rpm (pillar): (c) transversal section of sample (×50,000), with greater magnification (×90,000) for the central part of the analyzed region, (d) morphology of film (×100,000).

3.2. Pillar-type structures

A second type of film morphology occurs when the angle α remains fixed at 80°, but the substrate revolves at a speed $\dot{\phi} = 36.0$ rpm, which is considered high when compared to the deposition rate, (Fig. 5(c and d)). Under these conditions the film structures are of the pillar-type. One of the main characteristics of this type of film is its high level of porosity, bigger than the films structures of the helical-type, observed qualitatively in Fig. 5(b and d). The separation between columns is not uniform and varies between 10 and 50 nm. It results from the extreme oblique angle used in the deposition which enables the shadow effect to set in from the initial nucleation phase. During the process of film deposition the growth of the columns is interrupted by the shadow effect caused by neighboring columns, forcing the neighboring columns of each interrupted column to grow separately. In some cases the separation between columns occurring during growth appears at the beginning of film formation, as shown in the magnified version of Fig. 5(c). Contrary to what is observed for the helical-type structures, the top of the pillar-type structures show more rounded shapes, Fig. 5d. Fig. 6 shows pillar-type structures of WO_3 films deposited onto a W substrate.

Table 2
Structures expected to be formed during a 50 min deposition with a rotating substrate holder

Angular speed (rpm)	Number of turns	Radius (nm)	Column structure
0.042	∼2.0	53	Helical
36	1800	0.06	Pillar

3.3. Charge capacity

The WO_3/ITO and WO_3/W/ITO samples which were characterized using chronopotentiometry with potential limitation, had thickness of approximately 300 nm. This study is concerned with the electrochemical behavior of the structured samples. Fig. 7 shows the behavior of the potential of the samples as a function of time, in the first cycle of intercalation/deintercalation. The curves are monotonic with respect to time, which is a characteristic of amorphous thin films.

The results obtained for the volumetric charge capacities of the pillar-type, tilted-type, and helical-type thin film structures are presented in Fig. 8. The curves show a continuous decrease of the capacity, characteristic of intercalated materials. Such a decrease is generally associated with structural modifications of the film caused by ion trapping [31,32]. Taking as reference the electrochemical behavior of the tilted-type structures, the results of the charge capacity after 50 cycles present better performance in the following performance decreasing order: pillar/W/ITO, pillar/ITO, helical/ITO, and tilted/ITO. Therefore, there is a smaller loss of charge capacity in pillar-type structures. This may be associated with the larger porosity present in this type of structure. Among the pillar-type structures the best performance was achieved by the sample with deposition performed onto the W/ITO substrate. This result may be explained by the better structural behavior of the WO_3/W/ITO system during the intercalation/deintercalation cycles.

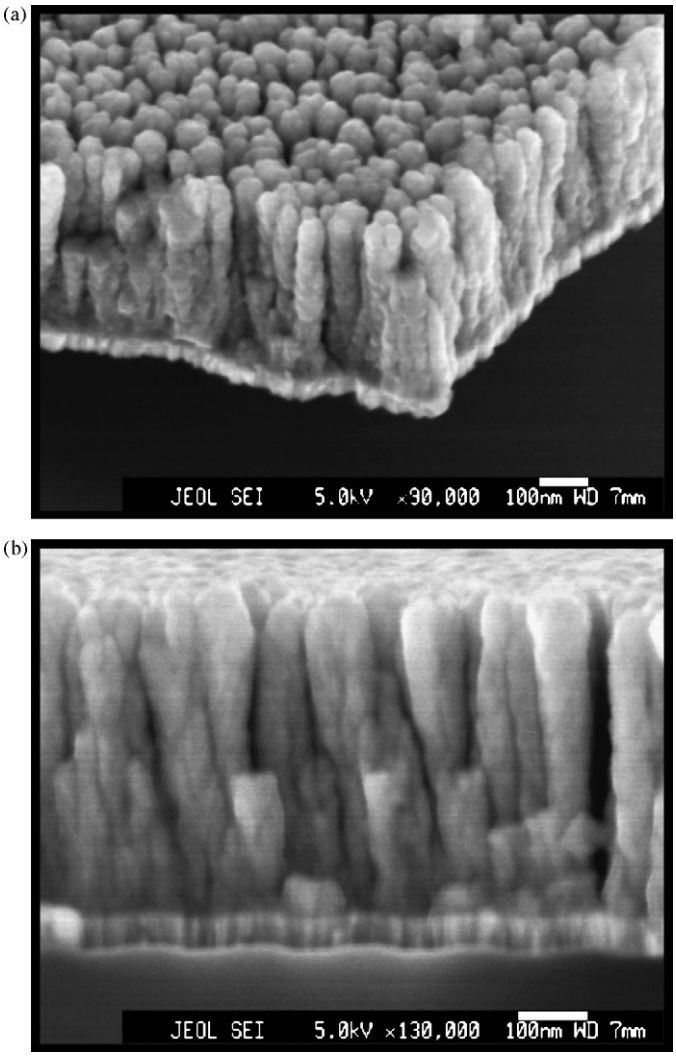

Fig. 6. Pillar-type structures of WO_3 film onto W/Si substrate, in the 100 nm scale (a) visualization in 3D (×90,000); (b) transversal section (×130,000).

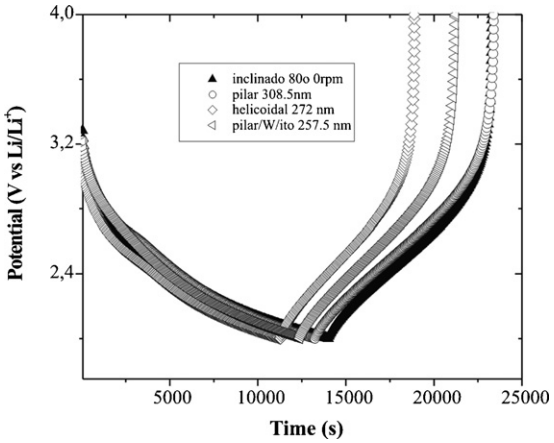

Fig. 7. Potential in the first cycle of intercalation/deintercalation of WO_3 films in their different types of structure.

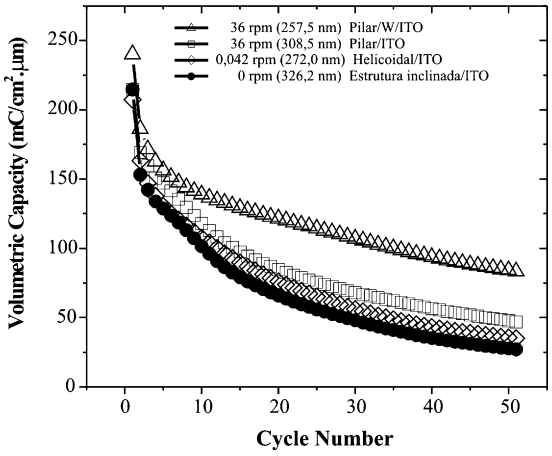

Fig. 8. Curve of charge capacity during 50 cycles, for WO_3 films with pillar-like structure onto W/ITO and ITO glass substrates (thicknesses 257.5 and 308.5 nm, respectively); helical structures (thickness 272 nm) and inclined structures (35°, 326.2 nm), onto ITO/glass substrate.

4. Conclusions

In summary, it was possible to deposit WO_3 pillar-type and helical-type structures by mainly controlling the substrate speed rotation. The pillar-type structures obtained under high speed (Fig. 5) show a higher degree of porosity than the films deposited conventionally with $\alpha = 0°$ and without rotation, Ref. [15]. Even in relation to samples deposited on substrates at an inclination angle $\alpha = 80°$ maintaining the substrate stationary. However, the porous characteristic did not grant a significant improvement on the charge capacity.

Thin films produced with a helical-type structure have a radial growth probably facilitated by the angular distribution of the incident flux and by the shape presented by the top of the columns in this type of structure.

An attempt to improve the interface WO_3/ITO was done by depositing first a tungsten film onto the ITO glass substrate which then served as a W substrate for the WO_3 pillar-type thin film structure.

As a result, after several intercalation/deintercalation cycles, the charge capacity practically doubled in comparison with a sample of similar thickness in which the deposition had occurred at a 80° angle with a stationary substrate.

Therefore, with an improvement in this type of interface, one may seek to build devices where one could benefit from the influence of porosity over the behavior of the charge capacity of structured thin films.

Acknowledgements

One author (R.F.) thanks CNPq (Brazil) for financial support. The SEM-FEG experiments were performed at the Laboratório Nacional de Luz Síncrotron (LNLS, Campinas, Brazil).

References

[1] M. Wakihara, Mater. Sci. Eng. R33 (2001) 109–134.
[2] J.M. Tarascon, M. Armand, Nature 414 (2001) 359–367.

[3] M. Winter, J.O. Besenhard, M.E. Spahr, Petr Nvák. Adv. Mater. 10 (1998) 725–763.
[4] A.G. Ritchie, J. Power Sources 96 (2001) 1–4.
[5] J.B. Bates, N.J. Dudney, B. Neudecker, A. Ueda, C.D. Evans, Solid State Ionics 135 (2000) 33–45.
[6] J.L. Souquet, M. Duclot, Solid State Ionics 148 (2002) 375–379.
[7] H. Katz, W. Bögel, J.-P. Büchel, J. Power Sources 72 (1998) 43–50.
[8] S.D. Jones, J.R. Akridge, F.K. Shokoohi, Solid State Ionics 69 (1994) 357–368.
[9] K. Brant, Solid State Ionics 69 (1994) 173–183.
[10] B. Dick, M.J. Brett, T.J. Smy, M.R. Freeman, M. Malac, R.F. Egerton, J. Vac. Sci. Technol. A 18 (2000) 1838–1844.
[11] J. Lintymer, J. Gaviolle, N. Martin, J. Takadoum, Surf. Coat. Tech. 174/175 (2003) 316–323.
[12] S.R. Kennedy, M.J. Brett, O. Toader, S. John, Nanoletters 2 (2002) 59–62.
[13] K. Robbie, M.J. Brett, J. Vac. Sci. Tech. A 15 (1997) 1460–1465.
[14] G. Zhang, Y. Zhao, J. Appl. Phys. 95 (2004) 267–271.
[15] R. Figueroa, M. Kleinke, T.G.S. Cruz, A. Gorenstein, J. Power Sources 162 (2006) 1351–1356.
[16] C.G. Granqvist, Electrochimica Acta 44 (1999) 3005–3015.
[17] P.R. Bueno, R.C. Faria, C.O. Avellaneda, E.R. Leite, L.O.S. Bulhões, Solid State Ionics 158 (2003) 415–426.
[18] K. Robbie, J.C. Sit, M.J. Brett, J. Vac. Sci. Tech. B 16 (1998) 1115–1122.
[19] D. Vick, T. Smy, M.J. Brett, J. Mater. Res. 17 (2002) 2904–2911.
[20] J.C. Sit, D. Vick, K. Robbie, M.J. Brett, J. Mater. Res. 14 (1999) 1197–1199.
[21] A.G. Dirks, H.J. Leamy, Thin solid films 47 (1977) 219–233.
[22] T. Karabacak, J.P. Singh, Y.-P. Zhao, G.-C. Wang, T.-M. Lu, Phys. Rev. B 68 (1–5) (2003) 125408.
[23] K.D. Harris, M.J. Brett, T.J. Smy, Christopher Backhouse. J. Electrochem. Soc. 147 (2000) 2002–2006.
[24] R.N. Tait, T. Smy, M.J. Brett, Thin Solid Films 226 (1993) 196–201.
[25] D. Vick, L.J. Friedrich, S.K. Dew, M.J. Brett, K. Robbie, M. Seto, T. Smy, Thin Solid Films 339 (1999) 88–94.
[26] R. Messier, T. Gehrke, C. Frankel, V.C. Venugopal, W. Otaño, A. Lakhtakia, J. Vac. Sci. Technol. A 15 (1997) 2148–2152.
[27] T. Karabacak, G.C. Wang, T.M. Lu, J. Vac. Sci. Technol. A 22 (2004) 1778–1784.
[28] D.-X. Ye, Y.-P. Zhao, G.-R. Yang, Y.-G. Zhao, G.-C. Wang, T.-M. Lu, Nanotechnology 13 (2002) 615–618.
[29] L.I. Maissel, R. Glang, Handbook of Thin Film technology, McGraw-Hill Book Company, 1970.
[30] O.R. Monteiro, Annu. Rev. Mater. Res 31 (2001) 111–137.
[31] Y. Sakurai, S. Okada, J. Yamaki, T. Okada, J. Power Sources 20 (1987) 173–177.
[32] J.-G. Zang, J.M. McGraw, J. Turner, D. Ginley, J. Electrochem. Soc. 144 (1997) 1630–1634.